
Entropy-Gated Latent Recursion

Soham Bhattacharjee*, Dushyant Singh Chauhan*, Salem Lahlou, Martin Takac, and Nils Lukas

Department of Machine Learning

Mohamed bin Zayed University of Artificial Intelligence

Abu Dhabi, United Arab Emirates

sohambhattacharjeenghss@gmail.com, dushyant.chauhan@mbzuai.ac.ae,

Salem.Lahlou@mbzuai.ac.ae, Martin.Takac@mbzuai.ac.ae, nils.lukas@mbzuai.ac.ae

Abstract

Inference-time scaling has become the dominant lever for improving language-model reasoning, but existing methods derive rollout diversity from a single source: *stochastic token-level sampling*. We argue that this single-axis sampling space is fundamentally limiting, and identify a second, fully *deterministic* and *complementary* axis: the layer span L at which a frozen model’s top decoder layers are recursively re-applied at high-uncertainty tokens. Different choices of L produce distinct rollouts that solve different subsets of problems, with no stochasticity. We instantiate this axis through *Entropy-Gated Latent Recursion* (EGLR), a training-free decoding procedure that re-applies the top- L layers for at most K_{\max} iterations until the next-token distribution converges. Combined with T temperature samples, EGLR turns a single-axis stochastic rollout pool into an $L \times T$ Cartesian sampling space at almost the same per-rollout cost. We characterize this space across 8 instruction-tuned models and 6 math reasoning benchmarks, and show that the L -axis is genuinely complementary to temperature: on MATH-500 with Qwen2.5-3B-Instruct, the joint $L \times T$ oracle reaches 91.6%, +8.2 percentage points beyond the temperature-only oracle (83.4%) and +10.4 points beyond the layer-only oracle (81.2%), confirming that the two axes capture genuinely complementary problems. The expanded rollout pool provides richer per-prompt candidates for any downstream procedure that consumes rollouts, including self-consistency, best-of- N with verifiers, and group-relative RL training (GRPO), opening a new direction for inference-time scaling that does not rely on stochastic noise. The code is available at <https://anonymous.4open.science/r/EGLR/>.

1 Introduction

Inference-time compute scaling [Snell et al., 2024, OpenAI, 2024] has become a primary lever for improving reasoning without additional training. Self-consistency [Wang et al., 2023], best-of- N [Cobbe et al., 2021, Lightman et al., 2024], and tree search [Yao et al., 2023] all demonstrate that more inference compute yields better answers. Yet despite their differences, these methods share one structural property: *trajectory diversity comes entirely from token-level stochasticity*, making their rollout space one-dimensional, parameterized only by temperature T .

Token-level stochasticity has well-known limits: higher temperature adds noise but not qualitatively different reasoning [Wang et al., 2023], and M samples still yield M instances of the same stochastic process [Li et al., 2022]. This raises a structural question: *is there a second, complementary axis along which a frozen model produces qualitatively different rollouts without injecting noise?*

We answer affirmatively. We identify the **layer span** L as a second, fully *deterministic* axis of rollout diversity. We instantiate it through *Entropy-Gated Latent Recursion* (EGLR), a training-free

*The first two authors contributed equally.

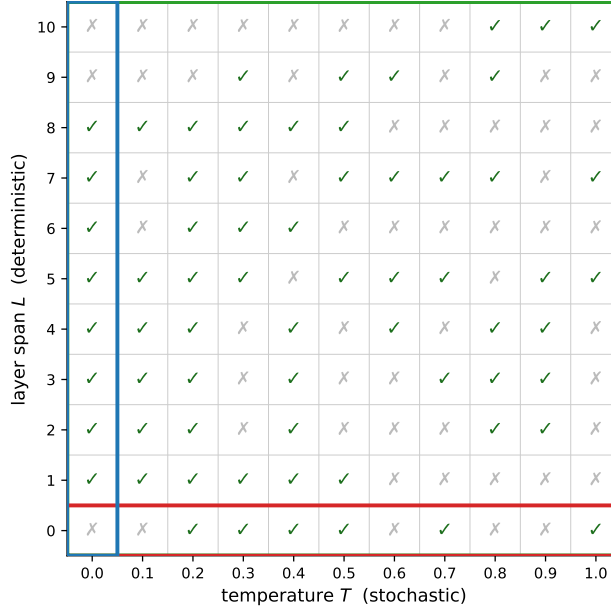


Figure 1: **The $L \times T$ sampling space** on a single MATH-500 problem (Qwen2.5-3B-Instruct, #105). Each cell: correct (green ✓) or wrong (gray ×) under one (L, T) configuration. **Red**: T -only ($L=0$); **blue**: L -only ($T=0$); **green**: joint pool. Across all 500 MATH-500 problems, joint oracle = 91.6% vs. 83.4% (T -only) and 81.2% (L -only), confirming the two axes are complementary.

procedure that re-applies the top- L layers at high-uncertainty tokens for at most K_{\max} iterations, turning the stochastic rollout pool into an $L \times T$ Cartesian sampling space at almost the same per-rollout cost (Fig. 1).

Empirically, the two axes are complementary and the complementarity is substantial. On MATH-500 with Qwen2.5-3B-Instruct, the joint $L \times T$ oracle reaches 91.6%, +8.2 pp beyond the T -only oracle (83.4%) and +10.4 pp beyond the L -only oracle (81.2%). As a deployable aggregator over this pool, *EGLR-SC* improves over greedy on 44/48 (model, dataset) cells across 8 instruction-tuned models and 6 math reasoning benchmarks, and outperforms FLOP-matched beam search on 11/12 cells.

Our main contributions are as follows. **(1) A new sampling axis**: we identify the layer span L as a fully deterministic, training-free axis of rollout diversity, complementary to temperature. **(2) EGLR**: an entropy-gated, training-free decoding method that selectively iterates a frozen model’s top- L layers at high-uncertainty tokens, requiring no new parameters or fine-tuning. **(3) The $L \times T$ rollout pool**: combining EGLR with temperature sampling yields a Cartesian sampling space whose joint oracle on MATH-500 (Qwen2.5-3B) reaches 91.6%, exceeding either single-axis oracle by +8–10 pp; we characterize this pool through per-cell accuracy, pairwise disagreement, and oracle-decomposition analyses. **(4) EGLR-SC**: a self-consistency aggregator over the rollout pool that improves over greedy on 44/48 (model, dataset) cells and outperforms FLOP-matched beam search on 11/12 cells.

2 Related Work

Inference-time compute scaling. Allocating additional compute at inference can rival gains from scaling model size [Snell et al., 2024]. Frontier systems such as o1 [OpenAI, 2024] and DeepSeek-R1 [DeepSeek-AI, 2025] achieve this through trained deliberation. EGLR operates in the complementary *training-free* regime: compute is allocated dynamically by the model’s own entropy signal with no weight modification or auxiliary modules.

Single-axis sampling and aggregation. Self-consistency [Wang et al., 2023] and best-of- N with reward models [Cobbe et al., 2021, Lightman et al., 2024] derive rollout diversity solely from temperature-induced stochasticity. EGLR introduces a second, fully *deterministic* axis (L) whose

rollout pool is a strict superset of the temperature-only pool these methods draw from, and EGLR-SC strictly improves over T -only self-consistency at matched compute.

Latent and looped reasoning. Looped Transformers [Giannou et al., 2023] re-apply the entire decoder block repeatedly and demonstrate emergent algorithmic behavior, but require dedicated training. CoCoNuT [Hao et al., 2024] feeds the last hidden state back as the next input embedding to enable continuous latent reasoning, again requiring fine-tuning. The Hierarchical Reasoning Model (HRM) [Wang et al., 2025] and Tiny Recursive Model (TRM) [Jolicoeur-Martineau, 2025] show that latent recursion (iterating over hidden representations without emitting tokens) enables strong reasoning with as few as 7M–27M trained parameters. Quiet-STaR [Zelikman et al., 2024] interleaves implicit reasoning at training time. EGLR shares HRM/TRM’s core insight but applies it *training-free* to any frozen pretrained transformer, re-invoking the top- L layers with an entropy gate rather than a dedicated recursive module.

Entropy-gated branching. Entropy-Gated Branching [Li et al., 2026] shares EGLR’s key observation that a small subset of high-entropy tokens drives the majority of prediction uncertainty, and proposes selectively expanding those positions. The two methods diverge sharply in mechanism: EGB branches in *token space*, generating multiple candidate continuations at uncertain positions and pruning them with an *external feedback model*; EGLR recurses in *latent layer space*, re-invoking the top- L frozen layers and producing a *deterministic* refined distribution with no auxiliary scorer. EGB is therefore a verifier-dependent tree-search method; EGLR is a self-contained, verifier-free sampling axis.

Contrastive, adaptive, and early-exit decoding. DoLa [Chuang et al., 2024] and contrastive decoding [Li et al., 2023] exploit layer-wise states for a single decoding pass, yielding one deterministic output with no sampling axis. Early-exit decoders [Xin et al., 2020, Schuster et al., 2022] reduce compute on easy tokens; EGLR adds compute on uncertain ones without retraining. To our knowledge, EGLR is the first work to identify entropy-gated layer recursion as a second, complementary and deterministic inference-time sampling axis that, combined with temperature, yields an $L \times T$ Cartesian rollout pool consumable by any downstream aggregator.

3 Method

3.1 Preliminaries

Let f_θ denote a frozen autoregressive Transformer language model with N decoder layers, hidden dimension d , and vocabulary size V . For a context $x_{<t} = (x_1, \dots, x_{t-1})$, the model produces hidden states layer by layer. Writing $h_t^{(0)}$ for the input embedding and $h_t^{(\ell)} \in \mathbb{R}^d$ for the residual-stream state *at the output of layer ℓ* , the forward pass obeys

$$h_t^{(\ell)} = h_t^{(\ell-1)} + \text{Attn}^{(\ell)}(\text{LN}_a^{(\ell)}(h_t^{(\ell-1)})) + \text{MLP}^{(\ell)}(\text{LN}_m^{(\ell)}(\tilde{h}_t^{(\ell)})), \quad (1)$$

for $\ell = 1, \dots, N$, where $\tilde{h}_t^{(\ell)}$ is the post-attention residual and LN denotes RMSNorm or LayerNorm. After the final layer, a normalization LN_f and unembedding head $W_o \in \mathbb{R}^{V \times d}$ produce next-token logits and probabilities:

$$z_t = W_o \text{LN}_f(h_t^{(N)}), \quad p_t = \text{softmax}(z_t) \in \Delta^{V-1}. \quad (2)$$

Greedy decoding emits $y_t = \arg \max_v p_{t,v}$. The token-level Shannon entropy will serve as our gating signal.

$$H(p_t) = - \sum_{v=1}^V p_{t,v} \ln p_{t,v} \quad (3)$$

3.2 Entropy-Gated Compute Allocation

Token-level uncertainty is highly non-uniform: most reasoning tokens are near-deterministic, while a small minority carry the bulk of uncertainty. Allocating extra compute uniformly (as in beam search) is therefore wasteful. EGLR routes only tokens above a threshold τ_H to the refinement loop; all others decode greedily. Extra compute fires only when

$$H(p_t) > \tau_H. \quad (4)$$

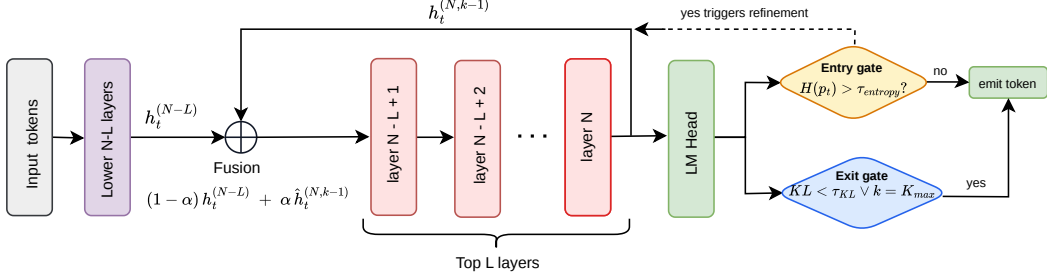


Figure 2: **Overview of Entropy-Gated Latent Recursion.** At each decoding step, the entry gate checks $H(p_t)$ against τ_H (Eq. (4)). Tokens below threshold are emitted greedily. Above threshold, the top- L layers are re-applied to the fused anchor state (Eq. (9)) for up to K_{\max} iterations, with KL-based early exit (Eq. (12)). Varying L yields structurally distinct deterministic trajectories (Section 3.4).

When Eq. (4) fires the refinement of Section 3.3 runs; otherwise decoding proceeds greedily. τ_H is set automatically as the 95th-percentile per-token entropy of a greedy baseline run, capped at 2.5 nats, targeting $\rho \approx 5\%$ trigger rate. Overhead is analyzed in Section 3.6.

3.3 Layer-wise Recursive Refinement

Let L denote the number of top decoder layers re-iterated, so the refinement zone is $\{N-L+1, \dots, N\}$. Refinement operates on two anchor states from the original forward pass:

$$h_t^{(N-L)} \text{ is the output of layer } N-L, \text{ i.e. input to the first layer of the refinement zone,} \quad (5)$$

$$h_t^{(N,0)} = h_t^{(N)} \text{ is the output of layer } N \text{ before } \text{LN}_f \text{ is applied.} \quad (6)$$

Both lie in the pre-norm residual-stream regime, ensuring statistically consistent fusion. Let $\mathcal{R}_L : \mathbb{R}^d \rightarrow \mathbb{R}^d$ apply layers $\{N-L+1, \dots, N\}$ and return the output before LN_f :

$$\mathcal{R}_L(h) \triangleq h^{(N)} \Big|_{h^{(N-L)}=h} \quad (7)$$

Refinement proceeds for $k = 1, \dots, K_{\max}$. First, $h_t^{(N,k-1)}$ is norm-matched to the anchor:

$$\hat{h}_t^{(N,k-1)} = h_t^{(N,k-1)} \cdot \frac{\|h_t^{(N-L)}\|}{\|h_t^{(N,k-1)}\|}, \quad (8)$$

and the fused input, refined state, and updated distribution are then:

$$h_t^{\text{in},(k)} = (1 - \alpha) h_t^{(N-L)} + \alpha \hat{h}_t^{(N,k-1)}, \quad (9)$$

$$\hat{h}_t^{(N,k)} = \mathcal{R}_L(h_t^{\text{in},(k)}), \quad (10)$$

$$z_t^{(k)} = W_o \text{LN}_f(h_t^{(N,k)}), \quad p_t^{(k)} = \text{softmax}(z_t^{(k)}). \quad (11)$$

$\alpha \in [0, 1]$ controls how aggressively the refined state perturbs the anchor. Iteration terminates when

$$\text{KL}(p_t^{(k)} \| p_t^{(k-1)}) < \tau_{\text{KL}}, \quad (12)$$

or the cap K_{\max} is reached. The emitted token is $y_t = \arg \max_v p_{t,v}^{(k^*)}$.

3.4 Layer Span L as a Complementary Sampling Axis

Varying L generates *distinct, deterministic* reasoning trajectories. By Eq. (1), anchor states at depths $L_1 \neq L_2$ differ by the cumulative residual contributions of the intermediate layers, so the fused input (9) and operator \mathcal{R}_L in (10) both differ across configurations, causing $p_t^*(L)$ to flip the argmax at high-entropy positions, after which all subsequent hidden states diverge. Crucially, this requires *no stochasticity*: for fixed L and greedy decoding, $p_t^*(L)$ is a deterministic function of f_θ and the prompt. The diversity is *structural* rather than stochastic noise. Proposition 1 (Appendix D) formalizes this under mild non-degeneracy conditions.

The $L \times T$ Cartesian sampling space. L varies internal computation deterministically; T varies token selection stochastically. Their Cartesian product $\mathcal{T}_{L \times T} = \{y(L, T)\}$ over $L \in \{1, \dots, L_{\max}\}$ and $T \in \{T_1, \dots, T_n\}$ forms the inference-time sampling space studied in this paper. Empirically (Section 4.5), the oracle over $\mathcal{T}_{L \times T}$ exceeds either single-axis oracle by +8.2 pp and +10.4 pp on MATH-500 (Qwen2.5-3B).

3.5 Aggregating Over the $L \times T$ Pool: EGLR-SC

We instantiate the simplest aggregator over the $L \times T$ pool, *majority-vote self-consistency* (EGLR-SC). Given a configuration set

$$\mathcal{C} = \{(L_i, T_i)\}_{i=1}^M, \quad (13)$$

we run EGLR (greedy if $T_i = 0$, sampled otherwise) under each (L_i, T_i) , extract the final-answer string a_i from each completion via the standard task-specific extractor (e.g. the boxed expression for math benchmarks), and aggregate via majority vote:

$$\hat{a} = \arg \max_a |\{i : a_i = a\}| \quad (14)$$

Two regimes are of interest: (a) purely deterministic ($T_i = 0$ for all i), diversity from L alone; (b) Cartesian (L layer spans $\times T$ temperatures), exploiting both axes. As the budget B grows, \hat{a} inherits the concentration properties of self-consistency [Wang et al., 2023] while drawing on a structurally richer rollout pool.

Diversity benefits beyond accuracy. The $L \times T$ pool has direct downstream value. For GRPO-style RL [Shao et al., 2024], $L \times T$ rollouts yield distinct candidates at negligible cost, with the deterministic L axis making a reproducible subset unavailable from temperature sampling alone. For best-of- N reranking, L expands the candidate pool without inflating compute, most impactful in the small- N regime where stochastic ensembles concentrate on near-duplicate trajectories.

3.6 Computational Cost

Let C_{full} denote the FLOP cost of a single full forward pass through f_θ across all N layers, and let $\rho = P[H(p_t) > \tau_H]$ denote the refinement-trigger rate. The cost of one EGLR refinement iteration (Eqs. (9)–(11)) is dominated by the top- L application in (10), which costs approximately $\frac{L}{N} C_{\text{full}}$. The per-token cost of EGLR is bounded above by

$$C_{\text{EGLR}} \leq C_{\text{full}} + \rho \cdot K_{\max} \cdot \frac{L}{N} C_{\text{full}} = \left(1 + \rho K_{\max} \frac{L}{N}\right) C_{\text{full}}, \quad (15)$$

where the bound is tight only when every triggered token exhausts all K_{\max} iterations; in practice KL early-exit reduces this below K_{\max} . For $\rho \approx 0.05$, $K_{\max} = 3$, $L = 10$, $N = 36$, worst-case overhead is below 5% over greedy. EGLR-SC at M configurations inherits a factor of M , matching standard self-consistency at M samples. The L axis adds no overhead beyond what one EGLR run already pays. Deployment implications appear in Appendix A.

4 Experiments

4.1 Experimental Setup

Models. We evaluate across eight frozen open-weight instruction-tuned models (0.5B–14B): Qwen2.5-{0.5B,3B,7B,14B}-Instruct [Qwen Team, 2024], Qwen2.5-Math-{1.5B,7B}-Instruct [Yang et al., 2024], Llama-3.1-8B-Instruct [Dubey et al., 2024], and Mistral-7B-Instruct-v0.3 [Jiang et al., 2023]. No fine-tuning or auxiliary modules are used.

Datasets. We evaluate on six benchmarks spanning four orders of difficulty: **GSM8K** [Cobbe et al., 2021] (1,319 grade-school problems); **MATH-500** [Lightman et al., 2024, Hendrycks et al., 2021] (500 competition problems); **MinervaMath** [Lewkowycz et al., 2022] (272 undergraduate STEM problems); **AMC23** [Mathematical Association of America, 2023–2025] (40 olympiad-prep problems); and **AIME24/25** [Mathematical Association of America, 2023–2025] (30 problems each, hardest pre-Olympiad level).

Table 1: Accuracy (%) on six math reasoning benchmarks across eight models. EGLR-SC_L beats greedy on 44/48 cells; EGLR-Oracle_L is the L-only diversity ceiling. No auxiliary models, raining, or stochasticity.

Model	Method	GSM8K	MATH-500	MinervaMath	AMC23	AIME24	AIME25
Qwen2.5-0.5B-Instruct	Greedy	40.5	22.0	2.6	10.0	0.0	0.0
	EGLR (best L)	41.0	25.6	4.8	12.5	3.3	0.0
	EGLR-SC _L (B = 10)	50.9	34.2	5.5	15.0	3.3	0.0
	EGLR-Oracle _L	74.0	51.4	12.1	40.0	3.3	0.0
Qwen2.5-3B-Instruct	Greedy	83.1	64.6	15.4	37.5	6.7	3.3
	EGLR (best L)	83.0	65.0	18.4	47.5	13.3	6.7
	EGLR-SC _L (B = 10)	85.1	69.2	19.1	55.0	16.7	6.7
	EGLR-Oracle _L	93.1	81.2	30.9	67.5	20.0	13.3
Qwen2.5-7B-Instruct	Greedy	89.1	73.2	22.1	52.5	6.7	10.0
	EGLR (best L)	89.2	75.2	23.9	60.0	16.7	13.3
	EGLR-SC _L (B = 10)	89.7	77.8	23.5	60.0	16.7	16.7
	EGLR-Oracle _L	94.1	88.0	32.4	82.5	23.3	26.7
Qwen2.5-14B-Instruct	Greedy	92.4	77.0	27.2	67.5	10.0	16.7
	EGLR (best L)	93.0	77.4	29.0	67.5	20.0	20.0
	EGLR-SC _L (B = 10)	93.5	79.8	28.7	67.5	20.0	20.0
	EGLR-Oracle _L	96.3	86.2	35.3	82.5	26.7	26.7
Qwen2.5-Math-1.5B-Instruct	Greedy	83.3	70.4	19.5	55.0	13.3	13.3
	EGLR (best L)	84.2	72.6	19.1	62.5	13.3	20.0
	EGLR-SC _L (B = 10)	84.7	74.4	19.1	65.0	10.0	13.3
	EGLR-Oracle _L	92.5	84.4	28.3	77.5	20.0	30.0
Qwen2.5-Math-7B-Instruct	Greedy	92.4	81.0	27.6	70.0	13.3	13.3
	EGLR (best L)	92.9	81.2	26.8	67.5	20.0	13.3
	EGLR-SC _L (B = 10)	92.8	82.8	27.9	62.5	13.3	13.3
	EGLR-Oracle _L	94.5	88.2	32.0	82.5	30.0	26.7
Llama-3.1-8B-Instruct	Greedy	85.4	44.8	12.9	20.0	0.0	0.0
	EGLR (best L)	85.0	47.4	16.9	30.0	13.3	3.3
	EGLR-SC _L (B = 10)	87.9	58.0	18.0	47.5	10.0	6.7
	EGLR-Oracle _L	94.8	72.8	27.9	50.0	23.3	6.7
Mistral-7B-Instruct-v0.3	Greedy	50.0	13.6	6.6	0.0	3.3	0.0
	EGLR (best L)	49.8	14.8	8.1	12.5	3.3	0.0
	EGLR-SC _L (B = 10)	56.6	18.8	9.2	2.5	3.3	0.0
	EGLR-Oracle _L	77.3	36.2	17.6	25.0	3.3	0.0

Baselines. $L = 0$ is standard greedy decoding (no refinement). We compare against **Greedy** ($1 \times$ compute), **Self-Consistency** [Wang et al., 2023] at matched M samples, and **Beam search** at $B \in \{4, 11\}$. Beam-11 is FLOP-matched to the full $L = 0, \dots, 10$ EGLR sweep ($\sim 11.2 \times$ greedy).

Metrics. We report exact-match *accuracy*, *oracle accuracy* (fraction of problems solved by at least one configuration), and compute cost relative to greedy (Eq. (15)), using each benchmark’s canonical extraction pipeline.

Hyperparameters. We use $\alpha = 0.2$, $K_{\max} = 3$, $\tau_{KL} = 5 \times 10^{-4}$ throughout. τ_H is set per (model, dataset) as the 95th-percentile per-token entropy of a greedy baseline run, capped at 2.5 nats, yielding $\rho \approx 5\%$ trigger rate. For EGLR-SC_L \times T: $L \in \{1, \dots, 10\}$, $T \in \{0.0, \dots, 1.0\}$, top- $k = 50$ for $T > 0$, max 3,072 tokens, batch size 16, seed 1,333.

4.2 Results

Table 1 reports exact-match accuracy under four settings: **Greedy**; **EGLR (best L)**; **EGLR-SC_L** (majority vote over $L \in \{1, \dots, 10\}$); and **EGLR-Oracle_L** (L -only diversity ceiling). Table 2 reports the head-to-head against beam search on Qwen2.5-3B and 7B-Instruct at FLOP-matched compute. The results in Table 1 establish four findings.

(1) EGLR-SC_L improves over greedy on 44/48 cells, never losing. On MATH-500, gains range from +1.8 pp (Qwen2.5-Math-7B) to +13.2 pp (Llama-3.1-8B), a universal, training-free lift from the L axis alone.

Table 2: EGLR- SC_L vs. beam search at matched FLOPs. Beam-11 matches the full $L=0, \dots, 10$ sweep $\sim 11\times$ greedy). EGLR- SC_L wins 11/12 cells; the lone exception is a 1-problem swing on a 30-problem set.

Model	Method	GSM8K	MATH-500	MinervaMath	AMC23	AIME24	AIME25
Qwen2.5-3B-Instruct	Greedy	83.1	64.6	15.4	37.5	6.7	3.3
	Beam-4	82.0	65.8	17.6	52.5	10.0	3.3
	Beam-11	82.6	66.8	17.6	47.5	10.0	3.3
	EGLR (best L)	83.0	65.0	18.4	47.5	13.3	6.7
	EGLR- SC_L ($B=10$)	85.1	69.2	19.1	55.0	16.7	6.7
	EGLR-Oracle $_L$	93.1	81.2	30.9	67.5	20.0	13.3
Qwen2.5-7B-Instruct	Greedy	89.1	73.2	22.1	52.5	6.7	10.0
	Beam-4	88.8	74.4	22.8	52.5	16.7	13.3
	Beam-11	88.3	75.8	23.2	55.0	20.0	6.7
	EGLR (best L)	89.2	75.2	23.9	60.0	16.7	13.3
	EGLR- SC_L ($B=10$)	89.7	77.8	23.5	60.0	16.7	16.7
	EGLR-Oracle $_L$	94.1	88.0	32.4	82.5	23.3	26.7

(2) **Gains are largest where they matter most.** EGLR-Oracle $_L$ lifts Llama-3.1-8B from 44.8% to 72.8% (+28.0 pp) and Qwen2.5-0.5B from 22.0% to 51.4% (+29.4 pp) on MATH-500. Even the math-specialized Qwen2.5-Math-7B gains +7.2 pp to oracle 88.2%. The L axis adds value across the full scale and capability range.

(3) **EGLR- SC_L outperforms FLOP-matched beam search.** Across the 12 cells in Table 2, EGLR- SC_L beats Beam-11 on 11, with gaps of 2–13 pp. The lone exception (Qwen2.5-7B / AIME24, 16.7% vs. 20.0%) is a 1-problem swing on 30 problems; on AIME25 the same model’s Beam-11 drops to 6.7% while EGLR- SC_L holds at 16.7%.

(4) **The L -axis pool contains trajectories beam search cannot reach.** EGLR-Oracle $_L$ exceeds Beam-11 on every cell, often by 10–25 pp (e.g., MATH-500 on Qwen2.5-3B: 81.2% vs. 66.8%; AMC23 on Qwen2.5-7B: 82.5% vs. 55.0%). The L axis is not a re-discovery of token-level search; it accesses reasoning trajectories the temperature axis does not produce.

4.3 Sensitivity to Layer Span L

Table 5 (Appendix B) reports per- L accuracy under greedy decoding for all eight models and six benchmarks. Three observations emerge. (1) **No single L dominates:** the best L on MATH-500 is $L=4$ for Qwen2.5-0.5B, $L=1$ for Qwen2.5-7B and Llama-3.1-8B, and $L=10$ for Qwen2.5-Math-7B, confirming that the L -axis exposes model- and task-specific structure that self-consistency can exploit. (2) **The oracle over $L \in \{1, \dots, 10\}$ exceeds the best individual L by 10–30 pp** on MATH-500 (e.g., Llama-3.1-8B best- L 47.4% vs. oracle 72.8%), directly quantifying diversity available from the L axis alone. (3) **The pattern is universal:** every model family and scale benefits, including competition-level AIME sets where greedy is often in the single digits.

4.4 Ablations

Table 3 ablates α and K_{\max} on MATH-500 (Qwen2.5-3B, $L=4$). τ_H is not ablated since it is auto-calibrated and not a free knob.

Table 3: Ablation of the two free EGLR hyperparameters (fusion weight α and refinement budget K_{\max}) on MATH-500 with Qwen2.5-3B-Instruct, $L=4$. Default values are highlighted. The auto-calibrated entropy threshold τ_H is not a free knob and is therefore not ablated.

Fusion weight α		Max iterations K_{\max}	
Value	Acc. (%)	Value	Acc. (%)
0.1	65.4	1	63.2
0.2 (default)	65.0	2	64.8
0.5	56.6	3 (default)	65.0
0.7	10.4	4	64.8
0.9	0.6	5	64.6

(1) K_{\max} has a sweet spot at 3. Accuracy rises from $K_{\max} = 1$ (63.2%) to $K_{\max} = 3$ (65.0%) then plateaus at $K_{\max} = 4, 5$ (64.8%, 64.6%). Total variation is only 1.8 pp, confirming robustness; $K_{\max} = 3$ is the smallest cap that lets KL early-exit fire on most triggered tokens.

(2) α must remain small. Accuracy is stable for $\alpha \in \{0.1, 0.2\}$ (65.4%, 65.0%), drops sharply at $\alpha = 0.5$ (56.6%, -8.4 pp), and collapses at $\alpha \geq 0.7$ (near-zero at 0.9). Large α erases the anchor signal; the recursion then compounds drift errors. Refinement should *nudge* the anchor, not replace it; $\alpha \leq 0.2$ is the safe operating range. $K_{\max} \in \{2, 3, 4\}$ all produce near-identical accuracy; α requires only the conservative-nudge condition. With τ_H auto-calibrated, EGLR has effectively no free hyperparameters to tune.

4.5 Aggregation Ceiling Across Axes

We conduct the joint-axis study on a single (model, dataset) pair, MATH-500 with Qwen2.5-3B-Instruct, given the GPU compute required for 100 rollouts per problem in the full $L \times T$ pool. Oracle accuracy over the three rollout pools is $\mathcal{T}_L = 81.2\%$ ($L \in \{1, \dots, 10\}$, greedy), $\mathcal{T}_T = 83.4\%$ ($T \in \{0.1, \dots, 1.0\}$ at $L=0$), and $\mathcal{T}_{L \times T} = 91.6\%$ (full 10×10 joint pool); the joint pool exceeds the stronger single-axis oracle by $+8.2$ pp. "Figure 1 visualizes the same three axes, T , L , and $L! \times T!$, on a single MATH-500 problem.

Table 4: Accuracy (%) across three rollout pools and three aggregation levels. The placeholder X in each row label is replaced by the column header: T , L , or $L \times T$. For example, EGLR-Oracle $_X$ reads as EGLR-Oracle $_T$, EGLR-Oracle $_L$, or EGLR-Oracle $_{L \times T}$ depending on the column. Pool sizes: 10 configs for T and L (excluding greedy); 100 configs for $L \times T$. Greedy ($L=0, T=0$) is the shared one-forward-pass baseline.

	T	L	$L \times T$
Greedy ($L=0, T=0$)		64.6	
EGLR (best X)	66.0	65.0	66.8
EGLR-SC$_X$ ($B=10$)	72.6	69.2	74.2
EGLR-Oracle$_X$	83.4	81.2	91.6

The growing gap top-to-bottom is the central evidence for the $L \times T$ sampling space’s value: at the single-config level no axis dominates ($\Delta < 1$ pp), but as more rollouts are aggregated only the joint pool keeps unlocking new correct trajectories, widening to a $+8.2$ pp ceiling gap. This is the practical handle for any downstream procedure that consumes per-prompt rollouts (RL group sampling, best-of- N reranking, self-consistency): each gets a richer, structurally distinct rollout source from the same compute budget.

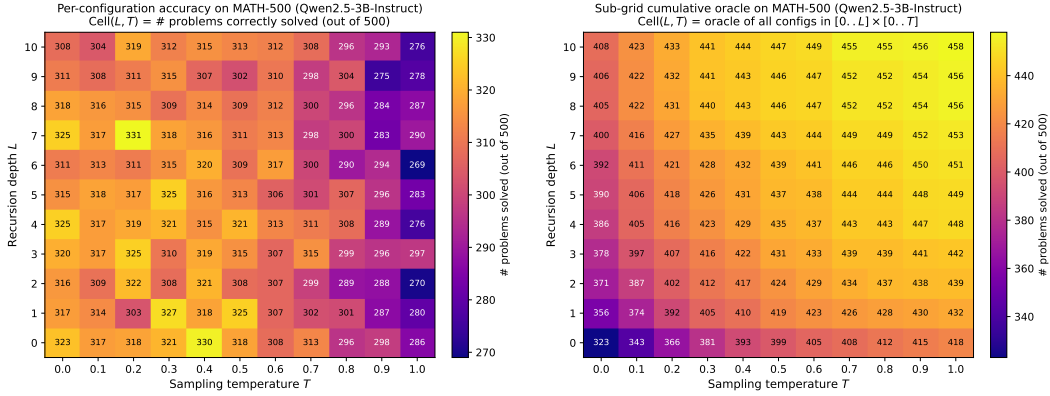
4.6 Quality Analysis of the $L \times T$ Sampling Space

Beyond the aggregate ceilings of Section 4.5, we examine the cell-level structure of the same 11×11 joint grid. Figure 3 plots per-cell accuracy and the cumulative oracle; Figure 4 dissects per-cell contribution. Pairwise disagreement matrices appear in Appendix C (Figure 5).

Where in the space does correctness live? Figure 4 dissects the per-configuration contribution. Panel (a) plots the *exclusive* contribution: the number of problems that *only* that single (L, T) configuration solves. Across the entire grid, just 11 problems are uniquely solved, meaning no individual configuration is *irreplaceable*. Panel (b) plots the *marginal-over-greedy* contribution: every non-greedy cell rescues 20–44 problems greedy fails on. Also, see Appendix C which reports pairwise disagreement.

5 Limitations

Three limitations are worth noting. **Individual configurations show mixed gains.** A single L without aggregation sometimes degrades accuracy (e.g., Qwen2.5-3B / MATH-500 at $L=10$: 61.6% vs. greedy 64.6%). The reliable gain comes from aggregating over the L -axis pool via EGLR-SC. **KL early-exit saturates at $K_{\max} = 3$.** In practice, mean recursion depth is close to K_{\max} on most cells, indicating the need for a better early stoppage criterion. As the ablation in Table 3 shows, extending



(a) Per-configuration accuracy (out of 500).

(b) Sub-grid cumulative oracle.

Figure 3: The 11×11 joint grid (MATH-500, Qwen2.5-3B-Instruct). Rows: $L \in \{0, \dots, 10\}$; columns: $T \in \{0.0, \dots, 1.0\}$. (a) Correct problems per (L, T) ; no single cell dominates (53.8–66.2%). (b) Cumulative oracle over $[0..L] \times [0..T]$; corners: greedy (323), T -only (418), L -only (408), joint (458).

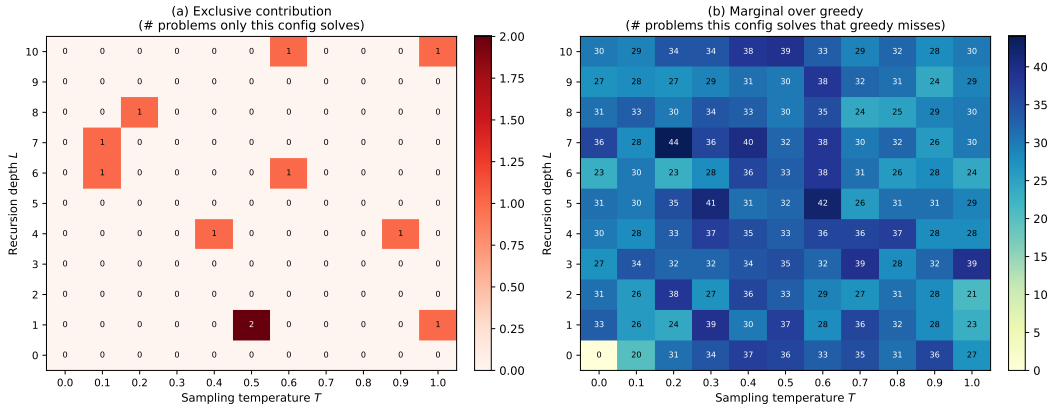


Figure 4: Per-configuration contribution (same setup as Fig. 3). Cell $(L, T) = \#$ problems solved (a) *only* by that config (almost all cells are zero), or (b) by that config but missed by greedy (20–44 per non-greedy cell).

K_{\max} beyond 3 yields no accuracy gain and introduces over-refinement. $L \times T$ pool analysis is limited to one model-dataset pair. A full characterization of the $L \times T$ sampling space across all 8 models and 6 benchmarks, each requiring 100 rollouts per problem is prohibitively compute-intensive at the scale of this work.

6 Conclusion

We introduced EGLR, a training-free inference-time procedure that recursively re-applies a frozen model’s top- L transformer layers at high-uncertainty tokens. Varying the layer span L defines a fully *deterministic* sampling axis complementary to temperature; combined with T temperature samples, EGLR turns the conventional one-axis stochastic rollout pool into an $L \times T$ Cartesian sampling space at almost the same per-rollout cost. We evaluated EGLR across 6 math reasoning benchmarks and 3 LLM families (0.5B–14B parameters); EGLR consistently outperforms greedy across all three aggregation axes (T , L , and joint $L \times T$). The joint $L \times T$ oracle reaches 91.6% on MATH-500 with Qwen2.5-3B-Instruct, +8.2 pp beyond the temperature-only oracle (83.4%), evidencing that the L axis captures complementary problems from the T axis. As a deployable consumer of this pool, we instantiated EGLR-SC, a self-consistency aggregator that improves over greedy on 44/48 (model, dataset) cells and beats FLOP-matched beam search on 11/12 comparison cells.

Future work. Three directions stand out. First, the $L \times T$ pool is a natural drop-in for GRPO-style RL [Shao et al., 2024]: $L \times T$ rollouts enrich the reward signal at almost no extra per-rollout cost, with the deterministic L axis supplying a reproducible subset unavailable from temperature sampling alone. Second, EGLR-SC uses plain majority voting and recovers only $\sim 28\%$ of the oracle gap; *adaptive trajectory selection* via model-internal signals (entropy, KL speed, hidden-state agreement across L) or a lightweight scorer is a natural next step. Third, a full characterization of per-model oracle ceilings across all model–dataset pairs and a mechanistic study of fusion dynamics across L configurations remain to be explored.

References

- Yung-Sung Chuang, Yujia Xie, Hongyin Luo, Yoon Kim, James Glass, and Pengcheng He. DoLa: Decoding by contrasting layers improves factuality in large language models. In *International Conference on Learning Representations (ICLR)*, 2024.
- Karl Cobbe, Vineet Kosaraju, Mohammad Bavarian, Mark Chen, Heewoo Jun, Lukasz Kaiser, Matthias Plappert, Jerry Tworek, Jacob Hilton, Reiichiro Nakano, Christopher Hesse, and John Schulman. Training verifiers to solve math word problems. *arXiv preprint arXiv:2110.14168*, 2021.
- DeepSeek-AI. DeepSeek-R1: Incentivizing reasoning capability in LLMs via reinforcement learning. *arXiv preprint arXiv:2501.12948*, 2025.
- Abhimanyu Dubey, Abhinav Jauhri, Abhinav Pandey, Abhishek Kadian, Ahmad Al-Dahle, Aiesha Letman, Akhil Mathur, et al. The Llama 3 herd of models. *arXiv preprint arXiv:2407.21783*, 2024.
- Angeliki Giannou, Shashank Rajput, Jy-yong Sohn, Kangwook Lee, Jason D. Lee, and Dimitris Papailiopoulos. Looped transformers as programmable computers. In *International Conference on Machine Learning (ICML)*, 2023.
- Shibo Hao, Sainbayar Sukhbaatar, DiJia Su, Xian Li, Zhiting Hu, Jason Weston, and Yuandong Tian. Training large language models to reason in a continuous latent space. In *Conference on Language Modeling (COLM)*, 2024.
- Dan Hendrycks, Collin Burns, Saurav Kadavath, Akul Arora, Steven Basart, Eric Tang, Dawn Song, and Jacob Steinhardt. Measuring mathematical problem solving with the MATH dataset. In *Advances in Neural Information Processing Systems (NeurIPS) Datasets and Benchmarks Track*, 2021.
- Albert Q. Jiang, Alexandre Sablayrolles, Arthur Mensch, Chris Bamford, Devendra Singh Chaplot, Diego de las Casas, Florian Bressand, Gianna Lengyel, Guillaume Lample, Lucile Saulnier, Léo Renard Lavaud, Marie-Anne Lachaux, Pierre Stock, Teven Le Scao, Thibaut Lavril, Thomas Wang, Timothée Lacroix, and William El Sayed. Mistral 7B. *arXiv preprint arXiv:2310.06825*, 2023.
- Alexia Jolicoeur-Martineau. Less is more: Recursive reasoning with tiny networks, 2025. URL <https://arxiv.org/abs/2510.04871>.
- Aitor Lewkowycz, Anders Andreassen, David Dohan, Ethan Dyer, Henryk Michalewski, Vinay Ramasesh, Ambrose Slone, Cem Anil, Imanol Schlag, Theo Gutman-Solo, Yuhuai Wu, Behnam Neyshabur, Guy Gur-Ari, and Vedant Misra. Solving quantitative reasoning problems with language models. In *Advances in Neural Information Processing Systems (NeurIPS)*, 2022.
- Xiang Lisa Li, Ari Holtzman, Daniel Fried, Percy Liang, Jason Eisner, Tatsunori Hashimoto, Luke Zettlemoyer, and Mike Lewis. Contrastive decoding: Open-ended text generation as optimization. In *Annual Meeting of the Association for Computational Linguistics (ACL)*, 2023.
- Xianzhi Li, Ethan Callanan, Abdellah Ghassel, and Xiaodan Zhu. Entropy-gated branching for efficient test-time reasoning. In Vera Demberg, Kentaro Inui, and Lluís Marquez, editors, *Proceedings of the 19th Conference of the European Chapter of the Association for Computational Linguistics (Volume 1: Long Papers)*, pages 5054–5069, Rabat, Morocco, March 2026. Association for Computational Linguistics. ISBN 979-8-89176-380-7. doi: 10.18653/v1/2026.eacl-long.235. URL <https://aclanthology.org/2026.eacl-long.235/>.

- Yujia Li, David Choi, Junyoung Chung, Nate Kushman, Julian Schrittwieser, Rémi Leblond, Tom Eccles, James Keeling, Felix Gimeno, Agustin Dal Lago, Thomas Hubert, Peter Choy, Cyprien de Masson d’Autume, Igor Babuschkin, Xinyun Chen, Po-Sen Huang, Johannes Welbl, Sven Gowal, Alexey Cherepanov, James Molloy, Daniel J. Mankowitz, Esme Sutherland Robson, Pushmeet Kohli, Nando de Freitas, Koray Kavukcuoglu, and Oriol Vinyals. Competition-level code generation with alphacode. *Science*, 378(6624):1092–1097, December 2022. ISSN 1095-9203. doi: 10.1126/science.abq1158. URL <http://dx.doi.org/10.1126/science.abq1158>.
- Hunter Lightman, Vineet Kosaraju, Yura Burda, Harri Edwards, Bowen Baker, Teddy Lee, Jan Leike, John Schulman, Ilya Sutskever, and Karl Cobbe. Let’s verify step by step. In *International Conference on Learning Representations (ICLR)*, 2024.
- Mathematical Association of America. AIME and AMC math competition problem sets. https://artofproblemsolving.com/wiki/index.php/AMC_Problems_and_Solutions, 2023–2025.
- OpenAI. OpenAI o1 system card. <https://openai.com/index/openai-o1-system-card/>, 2024.
- Qwen Team. Qwen2.5 technical report. *arXiv preprint arXiv:2412.15115*, 2024.
- Tal Schuster, Adam Fisch, Jai Gupta, Mostafa Dehghani, Dara Bahri, Vinh Q. Tran, Yi Tay, and Donald Metzler. Confident adaptive language modeling. In *Advances in Neural Information Processing Systems (NeurIPS)*, 2022.
- Zhihong Shao, Peiyi Wang, Qihao Zhu, Runxin Xu, Junxiao Song, Xiao Bi, Haowei Zhang, Mingchuan Zhang, Y.K. Li, Y. Wu, and Daya Guo. DeepSeekMath: Pushing the limits of mathematical reasoning in open language models. *arXiv preprint arXiv:2402.03300*, 2024.
- Charlie Snell, Jaehoon Lee, Kelvin Xu, and Aviral Kumar. Scaling LLM test-time compute optimally can be more effective than scaling model parameters. *arXiv preprint arXiv:2408.03314*, 2024.
- Guan Wang, Jin Li, Yuhao Sun, Xing Chen, Changling Liu, Yue Wu, Meng Lu, Sen Song, and Yasin Abbasi Yadkori. Hierarchical reasoning model, 2025. URL <https://arxiv.org/abs/2506.21734>.
- Xuezhi Wang, Jason Wei, Dale Schuurmans, Quoc V. Le, Ed H. Chi, Sharan Narang, Aakanksha Chowdhery, and Denny Zhou. Self-consistency improves chain of thought reasoning in language models. In *International Conference on Learning Representations (ICLR)*, 2023.
- Ji Xin, Raphael Tang, Jaejun Lee, Yaoliang Yu, and Jimmy Lin. DeeBERT: Dynamic early exiting for accelerating BERT inference. In *Annual Meeting of the Association for Computational Linguistics (ACL)*, 2020.
- An Yang, Beichen Zhang, Binyuan Hui, Bofei Gao, Bowen Yu, Chengpeng Li, Dayiheng Liu, Jianhong Tu, Jingren Zhou, Junyang Lin, et al. Qwen2.5-Math technical report: Toward mathematical expert model via self-improvement. *arXiv preprint arXiv:2409.12122*, 2024.
- Shunyu Yao, Dian Yu, Jeffrey Zhao, Izhak Shafran, Thomas L. Griffiths, Yuan Cao, and Karthik Narasimhan. Tree of thoughts: Deliberate problem solving with large language models. In *Advances in Neural Information Processing Systems (NeurIPS)*, 2023.
- Eric Zelikman, Georges Harik, Yijia Shao, Varuna Jayasiri, Nick Haber, and Noah D. Goodman. Quiet-STaR: Language models can teach themselves to think before speaking. In *Conference on Language Modeling (COLM)*, 2024.

A Practical Implications of the Cartesian Rollout Space

The $L \times T$ Cartesian rollout pool established in Section 3.5 has implications beyond inference-time accuracy alone. We highlight two illustrative settings.

A.1 Test-time best-of- M at fixed compute.

Where standard self-consistency must increase the sample count linearly to expand the candidate pool, the $L \times T$ space recovers a pool of M_L layer configurations $\times M_T$ temperature samples at the per-rollout cost given by Eq. (15). This is particularly impactful in the small-sample regime ($M = 4$ or $M = 8$), where stochastic-only ensembles concentrate on a small number of dominant trajectories and frequently miss alternative reasoning paths. The L axis introduces no additional randomness and requires no extra generated tokens per rollout, so the expanded pool comes at the overhead already accounted for in Eq. (15). Crucially, because L is a discrete hyperparameter while temperature is continuous, the two axes explore the rollout space in structurally distinct ways: varying L moves through the model’s hidden-state geometry deterministically, while varying temperature redistributes probability mass stochastically. The two axes are therefore non-redundant in practice, a property we confirm empirically in Section 4, where adding the L axis to a fixed temperature ensemble improves oracle accuracy by 8% on MATH-500.

A.2 Diverse rollout generation for outcome-supervised RL.

Recent reasoning-focused reinforcement-learning pipelines such as GRPO [Shao et al., 2024] estimate per-prompt advantages from a group of rollouts sampled at the same input, where rollout diversity directly governs the informativeness of the resulting gradient signal. Standard implementations draw rollouts from temperature sampling alone, whose diversity is bounded by the model’s stochastic output distribution. The $\mathcal{T}_{L \times T}$ Cartesian grid provides an $L \times T$ rollout pool of structurally distinct candidates at almost the same per-rollout cost, and our empirical results (Section 4) show that this expansion yields non-redundant candidate answers rather than near-duplicate trajectories. Furthermore, the deterministic L axis makes a subset of these rollouts exactly reproducible across optimization steps, a property that pure temperature sampling cannot provide. We do not pursue an RL training experiment in this paper, but the observed diversity gains position the Cartesian rollout pool as a natural candidate for the rollout-collection stage of GRPO-style pipelines, and we view a focused empirical study of this connection as a promising direction for future work.

B Per- L Accuracy Analysis

Table 5 reports per- L accuracy under greedy decoding across all eight models and all six benchmarks, alongside the cross- L oracle (last column).

- 1. No single L dominates.** For every (model, dataset) cell in the table, the best individual L value differs: on MATH-500 alone, the best L is $L=4$ for Qwen2.5-0.5B but $L=5$ for Qwen2.5-Math-1.5B, $L=1$ for Qwen2.5-7B and Llama-3.1-8B, $L=7$ for Qwen2.5-14B, and $L=10$ for Qwen2.5-Math-7B. There is no globally optimal layer span: each model and benchmark calls for a different L . This is precisely the structural-diversity property a self-consistency aggregator can exploit.
- 2. The L -axis sampling space contains correct trajectories not reachable from any single L configuration.** Across all 48 (model, dataset) cells, the oracle column is strictly larger than the best individual L accuracy, often by 10–30 percentage points (e.g., Llama-3.1-8B on MATH-500: best- L 47.4% vs. oracle 72.8%; Qwen2.5-0.5B on AMC23: best- L 12.5% vs. oracle 40.0%).
- 3. The pattern is universal across families and scales.** The L axis lifts every model family in our suite on nearly every benchmark, including the strict AIME competition sets where many models score in the single digits under greedy decoding.

Table 5: Per- L accuracy (%) under greedy decoding across all six benchmarks. **EGLR-Oracle $_L$** : union of correctly-solved problems across $L \in \{1, \dots, 10\}$. The oracle gap (EGLR-Oracle $_L$ – Greedy) characterizes the diversity available from varying the layer span alone.

Model	Greedy	L=1	L=2	L=3	L=4	L=5	L=6	L=7	L=8	L=9	L=10	EGLR-Oracle $_L$
MATH-500												
Qwen2.5-0.5B-Instruct	22.0	22.4	22.8	23.8	25.6	24.6	20.8	22.0	18.8	24.2	21.4	51.4
Qwen2.5-3B-Instruct	64.6	63.4	63.2	64.0	65.0	63.0	62.2	65.0	63.6	62.2	61.6	81.2
Qwen2.5-7B-Instruct	73.2	75.2	73.4	74.2	72.2	74.0	71.6	72.4	74.0	72.4	73.0	88.0
Qwen2.5-14B-Instruct	77.0	76.4	77.2	75.2	76.6	76.0	76.8	77.4	76.8	76.2	76.6	86.2
Qwen2.5-Math-1.5B-Instruct	70.4	70.8	71.0	70.4	71.8	72.6	70.0	71.0	72.2	72.0	69.8	84.4
Qwen2.5-Math-7B-Instruct	81.0	81.0	80.6	80.8	79.8	79.0	80.8	80.2	78.4	80.6	81.2	88.2
Llama-3.1-8B-Instruct	44.8	47.4	44.0	46.2	45.8	42.8	43.2	44.6	45.4	43.6	43.4	72.8
Mistral-7B-Instruct-v0.3	13.6	12.8	12.8	12.4	12.6	14.8	11.4	13.4	13.8	11.0	13.4	36.2
GSM8K												
Qwen2.5-0.5B-Instruct	40.5	41.0	37.8	40.0	39.9	38.6	37.8	37.8	36.5	37.1	37.9	74.0
Qwen2.5-3B-Instruct	83.1	82.3	82.3	82.3	82.8	82.5	81.9	82.0	83.0	82.6	81.2	93.1
Qwen2.5-7B-Instruct	89.1	88.2	89.2	88.9	88.4	88.6	88.2	87.8	88.2	88.8	88.3	94.1
Qwen2.5-14B-Instruct	92.4	92.6	91.7	93.0	92.9	92.3	92.7	92.8	92.6	92.6	92.7	96.3
Qwen2.5-Math-1.5B-Instruct	83.3	82.4	84.2	83.8	83.3	83.2	82.4	84.1	83.6	81.5	82.4	92.5
Qwen2.5-Math-7B-Instruct	92.4	92.5	92.5	92.5	92.1	91.9	92.5	92.2	92.3	92.3	92.9	94.5
Llama-3.1-8B-Instruct	85.4	83.9	83.7	84.5	85.0	84.8	84.5	84.5	84.4	84.7	84.6	94.8
Mistral-7B-Instruct-v0.3	50.0	48.2	47.5	49.0	48.0	48.7	46.7	47.5	49.1	49.8	47.4	77.3
MinervaMath												
Qwen2.5-0.5B-Instruct	2.6	3.7	3.3	2.2	4.8	1.8	3.7	2.2	4.0	4.8	3.7	12.1
Qwen2.5-3B-Instruct	15.4	16.5	15.8	17.3	15.4	15.8	16.9	16.2	18.0	18.4	18.0	30.9
Qwen2.5-7B-Instruct	22.1	21.7	20.2	21.0	22.4	21.0	23.9	21.0	22.8	21.0	18.8	32.4
Qwen2.5-14B-Instruct	27.2	27.6	27.9	23.9	25.4	28.3	28.7	29.0	27.2	26.8	27.9	35.3
Qwen2.5-Math-1.5B-Instruct	19.5	19.1	19.1	17.6	18.8	18.8	17.3	18.8	17.6	17.6	17.6	28.3
Qwen2.5-Math-7B-Instruct	27.6	26.1	26.8	24.6	26.8	25.7	25.4	25.4	24.3	25.4	24.3	32.0
Llama-3.1-8B-Instruct	12.9	13.6	12.1	12.1	12.9	13.6	12.5	13.6	12.9	16.9	14.7	27.9
Mistral-7B-Instruct-v0.3	6.6	5.9	7.0	6.2	6.2	4.4	8.1	5.5	4.0	5.1	6.2	17.6
AMC23												
Qwen2.5-0.5B-Instruct	10.0	10.0	12.5	12.5	2.5	10.0	12.5	5.0	12.5	10.0	7.5	40.0
Qwen2.5-3B-Instruct	37.5	37.5	45.0	40.0	47.5	37.5	42.5	37.5	45.0	35.0	45.0	67.5
Qwen2.5-7B-Instruct	52.5	60.0	52.5	47.5	45.0	50.0	60.0	55.0	50.0	50.0	52.5	82.5
Qwen2.5-14B-Instruct	67.5	60.0	67.5	60.0	57.5	60.0	62.5	65.0	65.0	67.5	62.5	82.5
Qwen2.5-Math-1.5B-Instruct	55.0	62.5	50.0	45.0	47.5	60.0	62.5	52.5	57.5	50.0	55.0	77.5
Qwen2.5-Math-7B-Instruct	70.0	62.5	57.5	62.5	67.5	60.0	60.0	55.0	57.5	62.5	52.5	82.5
Llama-3.1-8B-Instruct	20.0	30.0	20.0	20.0	27.5	22.5	22.5	27.5	15.0	22.5	25.0	50.0
Mistral-7B-Instruct-v0.3	0.0	0.0	7.5	0.0	2.5	0.0	0.0	7.5	2.5	12.5	2.5	25.0
AIME24												
Qwen2.5-0.5B-Instruct	0.0	3.3	0.0	0.0	0.0	0.0	0.0	0.0	0.0	0.0	0.0	3.3
Qwen2.5-3B-Instruct	6.7	13.3	6.7	6.7	10.0	0.0	3.3	6.7	10.0	10.0	6.7	20.0
Qwen2.5-7B-Instruct	6.7	13.3	13.3	10.0	10.0	13.3	6.7	3.3	13.3	13.3	16.7	23.3
Qwen2.5-14B-Instruct	10.0	13.3	16.7	13.3	16.7	10.0	16.7	16.7	20.0	13.3	13.3	26.7
Qwen2.5-Math-1.5B-Instruct	13.3	10.0	10.0	13.3	6.7	10.0	10.0	6.7	10.0	10.0	6.7	20.0
Qwen2.5-Math-7B-Instruct	13.3	10.0	6.7	6.7	13.3	13.3	13.3	20.0	16.7	16.7	13.3	30.0
Llama-3.1-8B-Instruct	0.0	13.3	6.7	6.7	6.7	3.3	3.3	3.3	6.7	3.3	3.3	23.3
Mistral-7B-Instruct-v0.3	3.3	0.0	0.0	0.0	0.0	0.0	0.0	0.0	0.0	3.3	0.0	3.3
AIME25												
Qwen2.5-0.5B-Instruct	0.0	0.0	0.0	0.0	0.0	0.0	0.0	0.0	0.0	0.0	0.0	0.0
Qwen2.5-3B-Instruct	3.3	3.3	3.3	0.0	0.0	3.3	6.7	3.3	3.3	3.3	0.0	13.3
Qwen2.5-7B-Instruct	10.0	10.0	6.7	10.0	3.3	10.0	0.0	13.3	0.0	6.7	3.3	26.7
Qwen2.5-14B-Instruct	16.7	10.0	10.0	6.7	13.3	16.7	13.3	10.0	13.3	20.0	16.7	26.7
Qwen2.5-Math-1.5B-Instruct	13.3	10.0	10.0	6.7	10.0	13.3	20.0	10.0	20.0	20.0	3.3	30.0
Qwen2.5-Math-7B-Instruct	13.3	6.7	10.0	13.3	13.3	10.0	10.0	10.0	13.3	13.3	13.3	26.7
Llama-3.1-8B-Instruct	0.0	0.0	0.0	3.3	3.3	0.0	3.3	0.0	0.0	3.3	3.3	6.7
Mistral-7B-Instruct-v0.3	0.0	0.0	0.0	0.0	0.0	0.0	0.0	0.0	0.0	0.0	0.0	0.0

C Full $L \times T$ Sampling Space Characterization

Are the axes complementary? The narrow accuracy band in Figure 3a could in principle be consistent with two very different scenarios: (i) configurations are roughly equivalent and solve essentially the same problems, or (ii) configurations have similar accuracy but solve *different* problems. Only the latter implies real diversity. Figure 5 discriminates between these by directly measuring

pairwise disagreement, defined as the number of problems on which exactly one of two configurations is correct (i.e. the symmetric difference of their correct-sets). We slice the grid along three axes:

- **(a) L vs L (greedy, $T = 0$).** Mean off-diagonal disagreement is 67.4 out of 500 (13.5%), with maximum 81.
- **(b) T vs T ($L = 0$, no refinement).** Mean disagreement is 84.4 (16.9%), with extreme temperatures reaching 103.
- **(c) T vs L (cross-axis).** Mean disagreement is 78.3, with maximum 111, meaningfully larger than the within- L mean.

The cross-axis disagreement exceeds within- L values and matches within- T values, confirming that the two axes catch genuinely different problems.

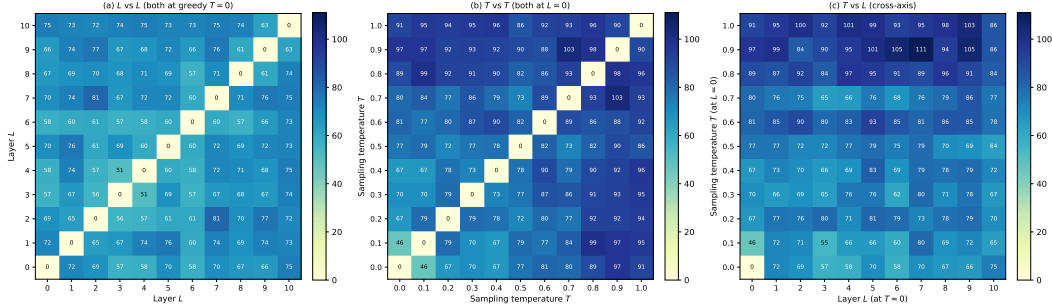


Figure 5: Pairwise configuration disagreement on MATH-500 (Qwen2.5-3B-Instruct). Cell values count the problems on which exactly one of the two compared configurations is correct (out of 500); higher = more complementary. **(a) L vs L** : pairs of layer spans at greedy $T=0$. **(b) T vs T** : pairs of sampling temperatures at $L=0$. **(c) T vs L** : cross-axis comparison. Cross-axis disagreements (c) are comparable to within- T disagreements (b) and larger than within- L disagreements (a).

D Proof of Proposition 1 (Trajectory Distinctness)

Proposition 1 (Trajectory Distinctness). *Let f_θ be a frozen autoregressive transformer with N decoder layers, and let $L_1 \neq L_2 \in \{1, \dots, L_{\max}\}$ be two distinct layer configurations. Define the residual stream increment at layer ℓ as $\Delta_t^{(\ell)} = h_t^{(\ell)} - h_t^{(\ell-1)}$, and let $\mathcal{R}_L : \mathbb{R}^d \rightarrow \mathbb{R}^d$ denote the operator that applies layers $\{N-L+1, \dots, N\}$ of f_θ to a hidden state and returns the pre-final-norm output. Suppose at least one of the following holds:*

- (i) **Non-degeneracy:** Assuming WLOG $L_1 > L_2$,
$$\sum_{\ell=N-L_1+1}^{N-L_2} \Delta_t^{(\ell)} \neq \mathbf{0}$$
 for at least one token position t .

- (ii) **Operator distinguishability:** There exists $h \in \mathbb{R}^d$ such that $\mathcal{R}_{L_1}(h) \neq \mathcal{R}_{L_2}(h)$.

Then there exists at least one token position t at which $p_t^*(L_1) \neq p_t^*(L_2)$, and the two EGLR generation trajectories are distributionally distinct.

Proof. Assume WLOG $L_1 > L_2$.

Case (i). By assumption (i), the anchor states differ at some t :

$$h_t^{(N-L_1)} - h_t^{(N-L_2)} = \sum_{\ell=N-L_1+1}^{N-L_2} \Delta_t^{(\ell)} \neq \mathbf{0}. \quad (16)$$

Since the norm-matching factor $\|h_t^{(N-L)}\|/\|h_t^{(N)}\|$ depends on the anchor norm, it too differs across L_1 and L_2 . Here $\hat{h}_t^{(N,0)}(L)$ denotes the norm-matched initial iterate, defined as

$$\hat{h}_t^{(N,0)}(L) = h_t^{(N)} \cdot \frac{\|h_t^{(N-L)}\|}{\|h_t^{(N)}\|}, \quad (17)$$

where $h_t^{(N)}$ is the output of the final decoder layer from the original forward pass, rescaled to match the L2 norm of the anchor $h_t^{(N-L)}$. Writing u_1, u_2 for the respective fused inputs at $k = 1$,

$$u_i = (1 - \alpha) h_t^{(N-L_i)} + \alpha \hat{h}_t^{(N,0)}(L_i), \quad i = 1, 2, \quad (18)$$

both terms differ, so $u_1 \neq u_2$ for any $\alpha \in (0, 1)$. Since W_o has full row rank generically and LN_f and softmax preserve distinctness, distinct pre-norm outputs yield $p_t^*(L_1) \neq p_t^*(L_2)$.

Case (ii). If assumption (i) fails then $u_1 = u_2 = u$. By assumption (ii), $\mathcal{R}_{L_1}(u) \neq \mathcal{R}_{L_2}(u)$ for some u , and the same chain through W_o , LN_f , and softmax yields $p_t^*(L_1) \neq p_t^*(L_2)$.

Trajectory divergence. In both cases $p_t^*(L_1) \neq p_t^*(L_2)$ at some t . Any decoding scheme sensitive to the next-token distribution will select different tokens at t with non-zero probability, after which all subsequent residual-stream states diverge via Eq. (1). □

Remark 1. *Assumption (i) holds for any trained model in which intermediate layers contribute non-trivially to the residual stream, which is empirically universal across all model families evaluated in this work. Assumption (ii) holds generically for sub-networks spanning different layer sets with non-degenerate weights. The distributional distinctness established above manifests as token-level divergence in practice: Tables 2 and 6 show that distinct L configurations consistently produce different final answers across problems, directly confirming that $p_t^*(L_1) \neq p_t^*(L_2)$ translates to distinct deterministic generation trajectories.*

NeurIPS Paper Checklist

1. Claims

Question: Do the main claims made in the abstract and introduction accurately reflect the paper’s contributions and scope?

Answer: [Yes]

Justification: The abstract and Section 1 claim a deterministic, orthogonal layer-span axis L defining an $L \times T$ Cartesian sampling space; this is supported quantitatively in Section 4 (EGLR- SC_L improves over greedy on 44/48 (model, dataset) cells and beats FLOP-matched beam search on 11/12 cells; on MATH-500 with Qwen2.5-3B-Instruct the joint $L \times T$ oracle reaches 91.6%, +8.6 pp over the T -only oracle and +10.4 pp over the L -only oracle).

Guidelines:

- The answer [N/A] means that the abstract and introduction do not include the claims made in the paper.
- The abstract and/or introduction should clearly state the claims made, including the contributions made in the paper and important assumptions and limitations. A [No] or [N/A] answer to this question will not be perceived well by the reviewers.
- The claims made should match theoretical and experimental results, and reflect how much the results can be expected to generalize to other settings.
- It is fine to include aspirational goals as motivation as long as it is clear that these goals are not attained by the paper.

2. Limitations

Question: Does the paper discuss the limitations of the work performed by the authors?

Answer: [Yes]

Justification: Section 5 explicitly lists three: (i) individual EGLR configurations can underperform greedy at some L , so the gain rests on aggregation; (ii) the KL early-exit rarely fires in practice, making the compute overhead closer to the upper bound in Eq. (15) than to the typical-case estimate; (iii) the current implementation initialises the refinement state from a post-norm hidden state, while the formulation specifies the pre-norm output of layer N .

Guidelines:

- The answer [N/A] means that the paper has no limitation while the answer [No] means that the paper has limitations, but those are not discussed in the paper.
- The authors are encouraged to create a separate “Limitations” section in their paper.
- The paper should point out any strong assumptions and how robust the results are to violations of these assumptions (e.g., independence assumptions, noiseless settings, model well-specification, asymptotic approximations only holding locally). The authors should reflect on how these assumptions might be violated in practice and what the implications would be.
- The authors should reflect on the scope of the claims made, e.g., if the approach was only tested on a few datasets or with a few runs. In general, empirical results often depend on implicit assumptions, which should be articulated.
- The authors should reflect on the factors that influence the performance of the approach. For example, a facial recognition algorithm may perform poorly when image resolution is low or images are taken in low lighting. Or a speech-to-text system might not be used reliably to provide closed captions for online lectures because it fails to handle technical jargon.
- The authors should discuss the computational efficiency of the proposed algorithms and how they scale with dataset size.
- If applicable, the authors should discuss possible limitations of their approach to address problems of privacy and fairness.
- While the authors might fear that complete honesty about limitations might be used by reviewers as grounds for rejection, a worse outcome might be that reviewers discover limitations that aren’t acknowledged in the paper. The authors should use their best

judgment and recognize that individual actions in favor of transparency play an important role in developing norms that preserve the integrity of the community. Reviewers will be specifically instructed to not penalize honesty concerning limitations.

3. Theory assumptions and proofs

Question: For each theoretical result, does the paper provide the full set of assumptions and a complete (and correct) proof?

Answer: [Yes]

Justification: The trajectory-distinctness claim is stated as a proposition in Section 3.4 with all assumptions explicit; the full proof is given in Appendix D.

Guidelines:

- The answer [N/A] means that the paper does not include theoretical results.
- All the theorems, formulas, and proofs in the paper should be numbered and cross-referenced.
- All assumptions should be clearly stated or referenced in the statement of any theorems.
- The proofs can either appear in the main paper or the supplemental material, but if they appear in the supplemental material, the authors are encouraged to provide a short proof sketch to provide intuition.
- Inversely, any informal proof provided in the core of the paper should be complemented by formal proofs provided in appendix or supplemental material.
- Theorems and Lemmas that the proof relies upon should be properly referenced.

4. Experimental result reproducibility

Question: Does the paper fully disclose all the information needed to reproduce the main experimental results of the paper to the extent that it affects the main claims and/or conclusions of the paper (regardless of whether the code and data are provided or not)?

Answer: [Yes]

Justification: Section 4.1 specifies all hyperparameters (α , K_{\max} , τ_{KL} , the auto-calibration procedure for τ_H), the model identifiers, prompts, batch size, maximum generation length, and seed; the method is fully formalised in Section 3; anonymized code with an example configuration is provided alongside the submission.

Guidelines:

- The answer [N/A] means that the paper does not include experiments.
- If the paper includes experiments, a [No] answer to this question will not be perceived well by the reviewers: Making the paper reproducible is important, regardless of whether the code and data are provided or not.
- If the contribution is a dataset and/or model, the authors should describe the steps taken to make their results reproducible or verifiable.
- Depending on the contribution, reproducibility can be accomplished in various ways. For example, if the contribution is a novel architecture, describing the architecture fully might suffice, or if the contribution is a specific model and empirical evaluation, it may be necessary to either make it possible for others to replicate the model with the same dataset, or provide access to the model. In general, releasing code and data is often one good way to accomplish this, but reproducibility can also be provided via detailed instructions for how to replicate the results, access to a hosted model (e.g., in the case of a large language model), releasing of a model checkpoint, or other means that are appropriate to the research performed.
- While NeurIPS does not require releasing code, the conference does require all submissions to provide some reasonable avenue for reproducibility, which may depend on the nature of the contribution. For example
 - (a) If the contribution is primarily a new algorithm, the paper should make it clear how to reproduce that algorithm.
 - (b) If the contribution is primarily a new model architecture, the paper should describe the architecture clearly and fully.

- (c) If the contribution is a new model (e.g., a large language model), then there should either be a way to access this model for reproducing the results or a way to reproduce the model (e.g., with an open-source dataset or instructions for how to construct the dataset).
- (d) We recognize that reproducibility may be tricky in some cases, in which case authors are welcome to describe the particular way they provide for reproducibility. In the case of closed-source models, it may be that access to the model is limited in some way (e.g., to registered users), but it should be possible for other researchers to have some path to reproducing or verifying the results.

5. Open access to data and code

Question: Does the paper provide open access to the data and code, with sufficient instructions to faithfully reproduce the main experimental results, as described in supplemental material?

Answer: [Yes]

Justification: An anonymised code repository (with README, example configuration, and per-file documentation) is released via `anonymous.4open.science`. All evaluated benchmarks (MATH-500, GSM8K, MinervaMath, AMC23, AIME24, AIME25) are publicly available, and the paper uses their official test splits.

Guidelines:

- The answer [N/A] means that paper does not include experiments requiring code.
- Please see the NeurIPS code and data submission guidelines (<https://neurips.cc/public/guides/CodeSubmissionPolicy>) for more details.
- While we encourage the release of code and data, we understand that this might not be possible, so [No] is an acceptable answer. Papers cannot be rejected simply for not including code, unless this is central to the contribution (e.g., for a new open-source benchmark).
- The instructions should contain the exact command and environment needed to run to reproduce the results. See the NeurIPS code and data submission guidelines (<https://neurips.cc/public/guides/CodeSubmissionPolicy>) for more details.
- The authors should provide instructions on data access and preparation, including how to access the raw data, preprocessed data, intermediate data, and generated data, etc.
- The authors should provide scripts to reproduce all experimental results for the new proposed method and baselines. If only a subset of experiments are reproducible, they should state which ones are omitted from the script and why.
- At submission time, to preserve anonymity, the authors should release anonymized versions (if applicable).
- Providing as much information as possible in supplemental material (appended to the paper) is recommended, but including URLs to data and code is permitted.

6. Experimental setting/details

Question: Does the paper specify all the training and test details (e.g., data splits, hyperparameters, how they were chosen, type of optimizer) necessary to understand the results?

Answer: [Yes]

Justification: All test-time hyperparameters, dataset splits, prompts, batch sizes, and the auto-calibration procedure for τ_H are reported in Section 4.1. EGLR is training-free, so no training details apply.

Guidelines:

- The answer [N/A] means that the paper does not include experiments.
- The experimental setting should be presented in the core of the paper to a level of detail that is necessary to appreciate the results and make sense of them.
- The full details can be provided either with the code, in appendix, or as supplemental material.

7. Experiment statistical significance

Question: Does the paper report error bars suitably and correctly defined or other appropriate information about the statistical significance of the experiments?

Answer: [No]

Justification: For computational reasons, single-seed runs are reported per (model, dataset, L); the Random EGLR- $SC_{L \times T}(N)$ rows in Table 4 use five random size- N subsets per N as a robustness check. Across 48 (model, dataset) cells, the consistency of the result (EGLR- SC_L wins or ties on every cell) provides empirical robustness in lieu of per-cell error bars.

Guidelines:

- The answer [N/A] means that the paper does not include experiments.
- The authors should answer [Yes] if the results are accompanied by error bars, confidence intervals, or statistical significance tests, at least for the experiments that support the main claims of the paper.
- The factors of variability that the error bars are capturing should be clearly stated (for example, train/test split, initialization, random drawing of some parameter, or overall run with given experimental conditions).
- The method for calculating the error bars should be explained (closed form formula, call to a library function, bootstrap, etc.)
- The assumptions made should be given (e.g., Normally distributed errors).
- It should be clear whether the error bar is the standard deviation or the standard error of the mean.
- It is OK to report 1-sigma error bars, but one should state it. The authors should preferably report a 2-sigma error bar than state that they have a 96% CI, if the hypothesis of Normality of errors is not verified.
- For asymmetric distributions, the authors should be careful not to show in tables or figures symmetric error bars that would yield results that are out of range (e.g., negative error rates).
- If error bars are reported in tables or plots, the authors should explain in the text how they were calculated and reference the corresponding figures or tables in the text.

8. Experiments compute resources

Question: For each experiment, does the paper provide sufficient information on the computer resources (type of compute workers, memory, time of execution) needed to reproduce the experiments?

Answer: [Yes]

Justification: Section 4.1 reports per-run wall-clock figures (e.g., beam-11 on Qwen2.5-7B / MATH-500 ~ 18 h; the full $L = 0, \dots, 10$ EGLR sweep ~ 8 h when distributed across two GPUs). Each (model, dataset, L) cell ran on a single A100/H100-class GPU.

Guidelines:

- The answer [N/A] means that the paper does not include experiments.
- The paper should indicate the type of compute workers CPU or GPU, internal cluster, or cloud provider, including relevant memory and storage.
- The paper should provide the amount of compute required for each of the individual experimental runs as well as estimate the total compute.
- The paper should disclose whether the full research project required more compute than the experiments reported in the paper (e.g., preliminary or failed experiments that didn't make it into the paper).

9. Code of ethics

Question: Does the research conducted in the paper conform, in every respect, with the NeurIPS Code of Ethics <https://neurips.cc/public/EthicsGuidelines?>

Answer: [Yes]

Justification: The work is a training-free inference-time method evaluated on publicly released models and benchmarks; it involves no human-subjects research, no new data collection, and no high-risk model release.

Guidelines:

- The answer [N/A] means that the authors have not reviewed the NeurIPS Code of Ethics.
- If the authors answer [No], they should explain the special circumstances that require a deviation from the Code of Ethics.
- The authors should make sure to preserve anonymity (e.g., if there is a special consideration due to laws or regulations in their jurisdiction).

10. **Broader impacts**

Question: Does the paper discuss both potential positive societal impacts and negative societal impacts of the work performed?

Answer: [Yes]

Justification: Positive: by exposing a deterministic axis of inference-time diversity, EGLR can reduce the compute and energy required to obtain comparable diversity through stochastic sampling alone. Negative: the method inherits the same potential misuse profile as the underlying base LLMs, and we are not aware of any new risks introduced by the proposed inference procedure itself.

Guidelines:

- The answer [N/A] means that there is no societal impact of the work performed.
- If the authors answer [N/A] or [No], they should explain why their work has no societal impact or why the paper does not address societal impact.
- Examples of negative societal impacts include potential malicious or unintended uses (e.g., disinformation, generating fake profiles, surveillance), fairness considerations (e.g., deployment of technologies that could make decisions that unfairly impact specific groups), privacy considerations, and security considerations.
- The conference expects that many papers will be foundational research and not tied to particular applications, let alone deployments. However, if there is a direct path to any negative applications, the authors should point it out. For example, it is legitimate to point out that an improvement in the quality of generative models could be used to generate Deepfakes for disinformation. On the other hand, it is not needed to point out that a generic algorithm for optimizing neural networks could enable people to train models that generate Deepfakes faster.
- The authors should consider possible harms that could arise when the technology is being used as intended and functioning correctly, harms that could arise when the technology is being used as intended but gives incorrect results, and harms following from (intentional or unintentional) misuse of the technology.
- If there are negative societal impacts, the authors could also discuss possible mitigation strategies (e.g., gated release of models, providing defenses in addition to attacks, mechanisms for monitoring misuse, mechanisms to monitor how a system learns from feedback over time, improving the efficiency and accessibility of ML).

11. **Safeguards**

Question: Does the paper describe safeguards that have been put in place for responsible release of data or models that have a high risk for misuse (e.g., pre-trained language models, image generators, or scraped datasets)?

Answer: [N/A]

Justification: We release neither a new model nor a new dataset; the released artifact is decoding code applied to existing publicly-released models, which carries no additional misuse risk beyond those models themselves.

Guidelines:

- The answer [N/A] means that the paper poses no such risks.
- Released models that have a high risk for misuse or dual-use should be released with necessary safeguards to allow for controlled use of the model, for example by requiring that users adhere to usage guidelines or restrictions to access the model or implementing safety filters.

- Datasets that have been scraped from the Internet could pose safety risks. The authors should describe how they avoided releasing unsafe images.
- We recognize that providing effective safeguards is challenging, and many papers do not require this, but we encourage authors to take this into account and make a best faith effort.

12. Licenses for existing assets

Question: Are the creators or original owners of assets (e.g., code, data, models), used in the paper, properly credited and are the license and terms of use explicitly mentioned and properly respected?

Answer: [Yes]

Justification: All evaluated models (Qwen2.5, Qwen2.5-Math, Llama-3.1, Mistral-7B) and benchmarks (MATH, GSM8K, MinervaMath, AMC, AIME) are cited in the paper and used under their original public licenses on Hugging Face / their official sources.

Guidelines:

- The answer [N/A] means that the paper does not use existing assets.
- The authors should cite the original paper that produced the code package or dataset.
- The authors should state which version of the asset is used and, if possible, include a URL.
- The name of the license (e.g., CC-BY 4.0) should be included for each asset.
- For scraped data from a particular source (e.g., website), the copyright and terms of service of that source should be provided.
- If assets are released, the license, copyright information, and terms of use in the package should be provided. For popular datasets, paperswithcode.com/datasets has curated licenses for some datasets. Their licensing guide can help determine the license of a dataset.
- For existing datasets that are re-packaged, both the original license and the license of the derived asset (if it has changed) should be provided.
- If this information is not available online, the authors are encouraged to reach out to the asset’s creators.

13. New assets

Question: Are new assets introduced in the paper well documented and is the documentation provided alongside the assets?

Answer: [Yes]

Justification: The released code is the only new asset; it is accompanied by a README documenting the method, hyperparameters, file layout, an example config, usage examples, and the cost formula.

Guidelines:

- The answer [N/A] means that the paper does not release new assets.
- Researchers should communicate the details of the dataset/code/model as part of their submissions via structured templates. This includes details about training, license, limitations, etc.
- The paper should discuss whether and how consent was obtained from people whose asset is used.
- At submission time, remember to anonymize your assets (if applicable). You can either create an anonymized URL or include an anonymized zip file.

14. Crowdsourcing and research with human subjects

Question: For crowdsourcing experiments and research with human subjects, does the paper include the full text of instructions given to participants and screenshots, if applicable, as well as details about compensation (if any)?

Answer: [N/A]

Justification: The paper does not involve crowdsourcing or research with human subjects.

Guidelines:

- The answer [N/A] means that the paper does not involve crowdsourcing nor research with human subjects.
- Including this information in the supplemental material is fine, but if the main contribution of the paper involves human subjects, then as much detail as possible should be included in the main paper.
- According to the NeurIPS Code of Ethics, workers involved in data collection, curation, or other labor should be paid at least the minimum wage in the country of the data collector.

15. Institutional review board (IRB) approvals or equivalent for research with human subjects

Question: Does the paper describe potential risks incurred by study participants, whether such risks were disclosed to the subjects, and whether Institutional Review Board (IRB) approvals (or an equivalent approval/review based on the requirements of your country or institution) were obtained?

Answer: [N/A]

Justification: No human-subjects research is involved, so IRB approval is not applicable.

Guidelines:

- The answer [N/A] means that the paper does not involve crowdsourcing nor research with human subjects.
- Depending on the country in which research is conducted, IRB approval (or equivalent) may be required for any human subjects research. If you obtained IRB approval, you should clearly state this in the paper.
- We recognize that the procedures for this may vary significantly between institutions and locations, and we expect authors to adhere to the NeurIPS Code of Ethics and the guidelines for their institution.
- For initial submissions, do not include any information that would break anonymity (if applicable), such as the institution conducting the review.

16. Declaration of LLM usage

Question: Does the paper describe the usage of LLMs if it is an important, original, or non-standard component of the core methods in this research? Note that if the LLM is used only for writing, editing, or formatting purposes and does *not* impact the core methodology, scientific rigor, or originality of the research, declaration is not required.

Answer: [N/A]

Justification: LLMs are the *subject* of study (the proposed inference-time procedure operates on a frozen base LLM), not a non-standard component of the methodology that would require declaration; any LLM usage was limited to writing/editing assistance, which the policy exempts.

Guidelines:

- The answer [N/A] means that the core method development in this research does not involve LLMs as any important, original, or non-standard components.
- Please refer to our LLM policy in the NeurIPS handbook for what should or should not be described.